이학박사 학위논문

Protective effect of zinc against A2E-induced toxicity in ARPE19 cells: Possible involvement of lysosomal acidification

zinc 의 조절에 의한 lysosomal acidification 의 회복을 통한 건성 연령 황반 변성에서의 치료효과

울산대학교 대학원

의 학 과

최 정 아

Protective effect of zinc against A2E-induced toxicity in ARPE19 cells: Possible involvement of lysosomal acidification

지 도 교 수　　윤 영 희

이 논문을 이학박사 학위 논문으로 제출함

2018 년 12 월

울 산 대 학 교 대 학 원

의　학　과

최 정 아

최정아의 이학박사학위 논문을 인준함

심사위원 고재영 (인)

심사위원 윤영희 (인)

심사위원 김양희 (인)

심사위원 이주용 (인)

심사위원 강민지 (인)

울 산 대 학 교 대 학 원

2018 년 12 월

Abstract

Dry age-related macular degeneration (AMD) is characterized by the accumulation of insoluble extracellular aggregates called drusen and the degeneration of photoreceptor cells and retinal pigment epithelium (RPE) cells. It has been proposed that dysfunctional lysosomes in the RPE cells contribute to the pathology of dry AMD by hindering the degradation of shed photoreceptor membranes. We have previously shown that raising the intracellular zinc levels can restore the lysosomal acidity and degradative functions of lysosomes. In the present study, we examined the effects of zinc on lysosomal alkalization and dysfunction in an *in vitro* model of AMD.

We used A2E (a lipofuscin derivative) to induce lysosomal dysfunction in a human RPE cell line (ARPE-19) and quantitatively assessed the A2E-induced cell death by measuring the amount of lactate dehydrogenase (LDH) released into the culture medium. The lysosomal pH of the cells treated with a zinc ionophore was measured using pHrodo™ Red-AM. In addition, we observed the effects of zinc on the lysosomal acidity and degradative functions in A2E-treated ARPE19 cells.

Twenty-four hours after A2E treatment, the ARPE19 cells showed a significant amount of cell death, increased A2E accumulation, and decreased pHrodo™ Red AM signals compared to the control cells. Moreover, the zinc

ionophore decreased the amount of A2E autofluorescence and restored the lysosomal pH to the acidic range. Following treatment of the ARPE19 cells with the zinc ionophore, A2E-induced cell death was significantly reduced.

These results support the possibility that adequate levels of zinc may help to overcome the cytotoxic effects of A2E or lysosomal alkalinizing agents, both of which may contribute to the pathogenesis of AMD.

Key words: Dry age-related macular degeneration (dry AMD), retinal pigment epithelium (RPE), lysosome, zinc, ARPE-19 cells

Contents

Figure contents

Introduction

Age-related macular degeneration (AMD) is the leading cause of irreversible vision loss in people over the age of 60. Macular degeneration is characterized by photoreceptor and retinal pigment epithelium (RPE) dysfunction[1, 2]. AMD can be classified as non-exudative (dry AMD) or exudative (wet AMD), depending on the presence or absence of neovascularization; dry AMD comprises about 90% of all AMD cases. The molecular hallmark of dry AMD is the accumulation of insoluble extracellular aggregates called drusen, which diminish the function of photoreceptor and RPE cells, thereby leading to decreased visual acuity[3-5].

Retinal pigment epithelial cells are among the most actively phagocytic cells in the body; they function to engulf shed photoreceptor outer segments (POS) and to recycle proteins and lipids[6]. The etiology and pathophysiology of macular degeneration are not well known, but previous reports have suggested the possible involvement of lysosomal pH dysregulation[7, 8]. The lysosomal dysfunction of the RPE cells leads to the accumulation of lipoprotein aggregates[9], which inhibit phagocytosis in the subretinal space and infiltrate the Bruch's membrane, and those that are retained impede essential cell functions[10]. Recently, studies have shown that the alkalization of lysosomes is one of the causes of AMD and that AMD may be attenuated by lysosomal reacidification[7, 11, 12].

In an effort to identify the mechanism underlying the restoration of an acidic lysosomal pH in chloroquine-treated RPE cells, Liu et al. utilized a screening approach to identify drugs capable of reacidifying lysosomes. In our recent study, clioquinol (ClioQ), a zinc ionophore, was effective for not only reacidifying the lysosomal pH but also overcoming the arrested autophagy induced by chloroquine in ARPE-19 (human RPE cell line) cells[13]. In the present study, we examined the effects of zinc on lysosomal alkalization and dysfunction in an in vitro and in vivo model of AMD.

Materials and Methods

Chemicals

N-retinylidene-N-retinylethanolamine (A2E) was obtained from two different companies, Gene and Cell Technologies (CA, USA) and Abta Bio (Seoul, Korea), due to A2E production and shipping problems. Concentrations of A2E that showed the same degree of fluorescence were used in the experiments. Chloroquine (CQ), clioquinol (ClioQ), $ZnCl_2$, and N,N,N′,N′,-tetrakis(2-pyridylmethyl)ethylenediamine (TPEN) were purchased from Sigma (St. Louis, MO, USA). 1H10 (AMPK inhibitor compound, zinc ionophore) was provided from Prof. Yang-Hee Kim of Sejong University (Seoul, Korea).

Cell culture

ARPE-19 cells were obtained from the American Type Culture Collection (CRL-2302; Manassas, VA, USA) and were cultured in medium (Dulbecco's Modified Eagle Medium Nutrient Mixture F-12; Invitrogen, Carlsbad, CA, USA) supplemented with 10% fetal bovine serum (FBS; Invitrogen) and 1% penicillin-streptomycin (Lonza, Allendale, NJ, USA) at 37°C in a humidified 5% CO2 incubator[14]. Cells were used after they reached approximately 80% confluence.

Western Blot Analysis

Cells and tissues were lysed in RIPA buffer (20 mM Tris-Cl pH 7.4, 150 mM NaCl, 1 mM EDTA, 1 mM EGTA, 1% Triton X-100, 2.5 mM sodium pyrophosphate, 1 μM Na_3VO_4, 1 μg/ml leupeptin, and 1 mM phenylmethylsulfonyl fluoride). The lysates were centrifuged and the protein concentration in the supernatants was determined using the Dc Protein Assay Reagent (Bio-Rad, Hercules, CA, USA). Samples with equal amounts of protein were separated by SDS-polyacrylamide gel electrophoresis (SDS-PAGE) and then transferred to PVDF membranes (Millipore, Bedford, MA, USA). Membranes were incubated overnight at 4°C with primary antibodies, followed by incubation with horseradish peroxidase-conjugated goat anti-rabbit IgG (1:10,000; Pierce). The following primary antibodies were used: anti-LC3 (1:1000, NOVUS, Littleton, CO, USA), anti-P62 (1:500, MBL, Des Plaines, IL, USA), and anti-β-actin (1:2500; Sigma).

Assessment of cell death

A2E-induced cell death was quantified by measuring the activity of lactate dehydrogenase (LDH) released into the culture medium. LDH activity was estimated using an automated microplate reader (UVmax; Molecular Devices, San Francisco, CA, USA) by measuring the rate of decrease in absorbance at 340 nm.

Immunocytochemistry

After fixation in 4% paraformaldehyde, cells were washed in PBS and incubated in a permeabilizing and blocking solution consisting of PBS containing 0.2% Triton X-100 and 1% bovine serum albumin (BSA). After incubation with primary antibody (LAMP-1, Abcam, 1:250) at 4°C for 24 h, cells were further incubated with Alexa Fluor-conjugated secondary antibodies (1:500; Invitrogen) and examined by confocal microscopy (Carl-Zeiss, Oberkochen, Germany).

Assessment of lysosomal pH using a confocal live-cell imaging system

ARPE-19 cells were grown to 60% confluence on glass-bottom dishes. Cells were stained with pHrodo™ Red AM intracellular pH indicator (Invitrogen) for 30 min at 37°C in a humidified 5% CO2 incubator and then transferred to a confocal live cell chamber. ARPE-19 cells were treated with A2E alone or with A2E combined with 1 μM ClioQ, 1 μM 1H10, or 1 μM ClioQ plus 0.5 μM TPEN. Confocal images were obtained using an LSM780 Confocal Live-Cell Imaging System (Carl Zeiss, Oberkochen, Germany).

Animals

The animal experiment protocol was approved by the Internal Review Board for Animal Experiments of Asan Life Science Institute, University of Ulsan College

of Medicine (Seoul, Korea). Male, 8 week-old (22-25 g) C57BL/6N mice were purchased from Orient Bio Inc. (Seoul, Korea), and maintained at 24°C ± 0.5°C under a 12 h light/dark cycle. We performed intraperitoneal (ip) injection of the animals or orally administered to them either chloroquine (10 mg/kg body weight in saline) or saline alone (control). CQ-induction was confirmed using a MICRONⅢ retinal imaging system (Phoenix Research Laboratories, Inc., Pleasanton, CA, USA).

TUNEL assay

In preparation for staining, the eyes were enucleated, embedded in O.C.T. compound (Tissue-Tek; Sakura Finetek, Torrance, CA, USA), cut into 10-μm-thick sections on a cryostat at -20°C, and mounted on pre-chilled glass slides coated with poly-L-lysine. The degree of apoptosis in the eye sections was determined by performing terminal deoxynucleotidyl transferase-mediated fluorescein-16-dUTP nick-end labeling (TUNEL) assays, as described by the manufacturer (Roche, Basel, Switzerland). Briefly, frozen sections were fixed with 4% PFA for 30 minutes at room temperature. After permeabilization with 0.1% Triton X-100 in distilled water containing 0.1% sodium citrate, sections were stained by incubation in a nucleotide mixture containing fluorescein-12-dUTP and terminal transferase (TdT) at 37°C for 60 minutes. Nuclei were counterstained with DAPI (4',6-diamidino-2-phenylindole)[15].

Immunohistochemistry

Retinal sections were prepared using a cryostat and placed onto glass slides. After fixation in 4% paraformaldehyde, the retinal section slides were washed in PBS and incubated in a permeabilizing and blocking solution consisting of PBS, 0.2% Triton X-100, and 1% bovine serum albumin (BSA). After incubation with anti-RPE65 (RPE, abcam, 1:250) or anti-rhodopsin (photoreceptor, Millipore, 1:250) primary antibody at 4°C for 24 hours, tissues were further incubated with Alexa Fluor-conjugated secondary antibodies (1:500; Invitrogen) and examined by LSM780 confocal microscopy (Carl-Zeiss).

Statistical analysis

All results are presented as mean ± SEM. Student's t-tests were used to evaluate the significance of differences among groups. Values of $P < 0.05$ were considered significant. All statistical analyses and graphical presentations were conducted and created using Sigma Plot version 10.0 software.

Results

Establishment of an *in vitro* model of AMD

For the establishment of an AMD model, we exposed ARPE-19 cells to A2E. Using A2E autofluorescence[16, 17], we confirmed the intensity of the autofluorescence over time using live-cell imaging. The A2E-treated ARPE-19 cells showed increased A2E accumulation (green dots) (Fig. 1). To observe the cytotoxicity, we exposed the cells to 1 to 10 μM of A2E for 24 h and measured the amount of LDH released into the medium. A2E accumulation caused the death of the ARPE-19 cells in a dose-dependent manner (Fig. 2).

A2E accumulation was localized to the lysosome and reduced the lysosomal acidity

To confirm the formation of an *in vitro* model of AMD and RPE denaturation with A2E, we observed A2E and lysosome co-localization using LAMP-1 staining. A2E accumulation gradually increased and largely overlapped with the LAMP-1 signals (Fig. 3A). Next, we examined the effect on the lysosomal pH. Lysosomal pH changes were estimated by staining the ARPE-19 cells with pHrodo™ Red AM, a pH-sensitive fluorescent dye, followed by observation with a confocal live-cell imaging system. The A2E-treated cells simultaneously showed

increased A2E fluorescence intensity and decreased fluorescence of pHrodo™ Red AM compared to the control cells (Fig. 3B, C).

Lysosome reacidification by zinc treatment in ARPE-19 cells

We performed live-cell imaging to examine the effect of zinc on the lysosomal pH using ClioQ or 1H10 as zinc ionophores (Supplement Fig. 1). Treatment with 1 μM of ClioQ or 1 μM of 1H10 caused the fluorescence intensity of pHrodo™ Red AM to markedly increase, indicating that the lysosomal pH was restored to the acidic range. Chelation of zinc with TPEN completely abolished the effect of ClioQ on the lysosomal pH, indicating that the acidification of the lysosome can be controlled by zinc (Fig. 4A, B). At the same time, treatment with 1 μM of ClioQ or 1 μM of 1H10 reduced the A2E accumulation in the ARPE-19 cells (Fig. 4A, C). Zinc restored the lysosomal pH to the acidic range, which led to increased lysosomal degradation.

Arrested autophagy from lysosomal dysfunction in A2E-treated ARPE-19 cells

With the enhanced lysosomal function, the autophagy pathway was activated to degrade abnormal protein aggregates in the ARPE-19 cells[13, 14]. After confirming that the accumulation of A2E in the RPE is associated with the lysosomal pH, we measured the autophagy flux in the ARPE-19 cells treated with A2E using

p62 as a marker[18]. When autophagy is arrested, the p62 levels increase. Western blot analysis with p62 showed increased protein levels in a dose-dependent manner, and analysis with LC3 showed that LC3-II also increased 3 h after treatment with A2E (Fig. 5A-C). Additionally, 1 μM of ClioQ or 1 μM of 1H10 reduced the p62 levels compared to A2E (Fig. 5D-F). These results indicated that the zinc-related lysosomal pH change restores the autophagic flux in A2E-treated ARPE-19 cells, in which the autophagic flux had been arrested.

Zinc reduced A2E accumulation and cytotoxicity in RPE cells

Next, we examined the protective effects of ClioQ and 1H10 on ARPE-19 cells. Following treatment with 1 μM of ClioQ or 1 μM of 1H10, decreased A2E accumulation was observed in the ARPE-19 cells (Fig. 6A). Additionally, the cell death induced by A2E accumulation was reduced with 1 μM ClioQ and ClioQ plus 500 nM zinc and in the 1 μM 1H10-treated cells, compared to the cells treated with 5 μM of A2E (Fig. 6B). The zinc ionophores substantially reduced the cell death induced by A2E.

Establishment of a CQ-induced AMD model in mice

According to our findings, alkalinization of the lysosomal pH can serve as a disease model for dry AMD, and CQ is one of the best known alkalinizing agents.

CQ triggers retinopathy as a consequence of the elevated lysosomal pH of RPE cells, resulting in the accumulation of lipofuscin-like material in both humans and animals that is characteristic of AMD[14, 19].

To establish an *in vivo* AMD model, we injected C57BL/6 mice with CQ. We administered chloroquine (10 mg/kg of body weight) or saline (control) daily to the animals through either ip or oral routes. After 10 weeks, we collected fundus photographs with a MICRON Ⅲ and performed immunohistochemistry. The CQ-injected mice showed an increase in the white or yellow dots, which appeared to be drusen, in the retina (Fig. 7A). The number of TUNEL-positive cells increased markedly in the retinal tissue of the mice that received ip injection or oral administration of CQ, compared to the retinal tissue of the saline-treated mice (Fig. 7B). In particular, the TUNEL-positive cells were observed to increase in the nuclear layer of the photoreceptor (outer nuclear layer, ONL) in the retinal tissue of both the mice treated with ip injection of CQ and those treated with oral administration of CQ. In the oral administration model, TUNEL-positive cell death was observed in the inner nuclear layer (INL) and the ganglion cell layer (GCL), as well as in the ONL. Furthermore, the RPE and photoreceptor cell layer had decreased levels of specific protein markers, compared to the levels in saline-treated mice (Fig. 7C). These results suggested that RPE damage from CQ in mice can serve as a disease model for dry AMD.

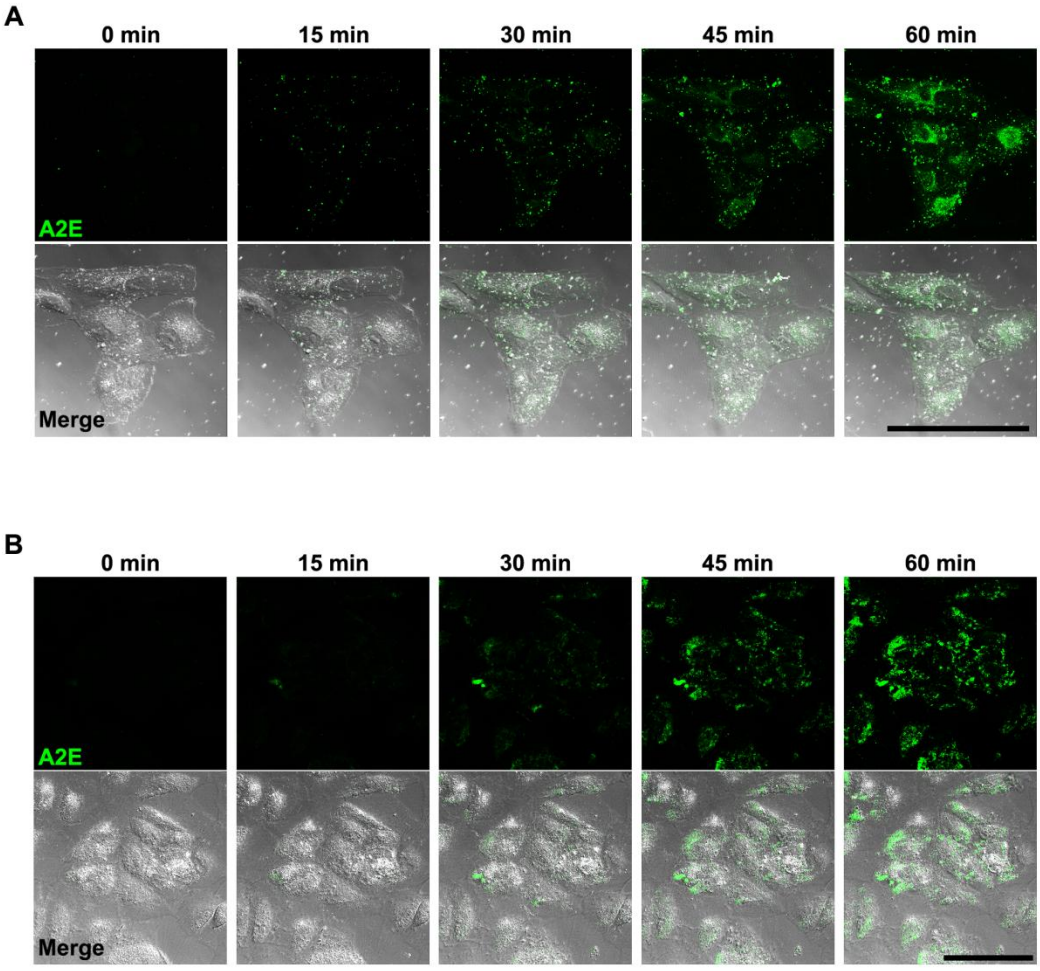

Figure 1. Establishment of an *in vitro* age-related macular degeneration model

After the addition of (A) 5 μM A2E (Gene and Cell Technologies) or (B) 50 μM A2E (Abtabio), the A2E accumulation (green dots) increased in the ARPE-19 cells, confirmed by confocal live-imaging using the LSM710 Confocal Live-Cell Imaging System. Original magnification, (A) × 630, (B) × 400; scale bar, 100 μm.

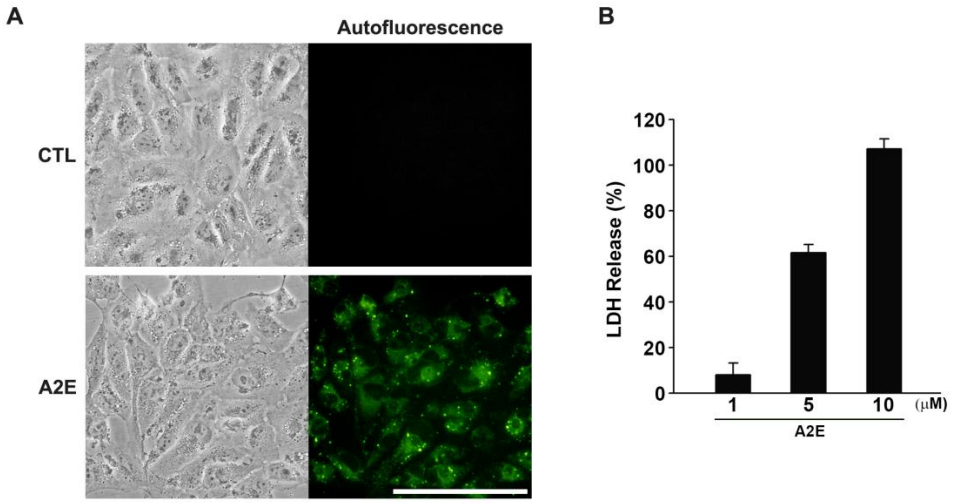

Figure 2. A2E accumulation induced the death of the ARPE-19 cells

(A) Phase contrast photomicrographs of the ARPE-19 cells (CTL, upper) and the

A

R

(B) Measurement of the LDH released into the medium of the ARPE-19 cells after

24 h of exposure to the indicated concentrations of A2E; the percentages are

expressed as the mean ± SD (*$P < 0.05$ compared to the controls, n = 3).

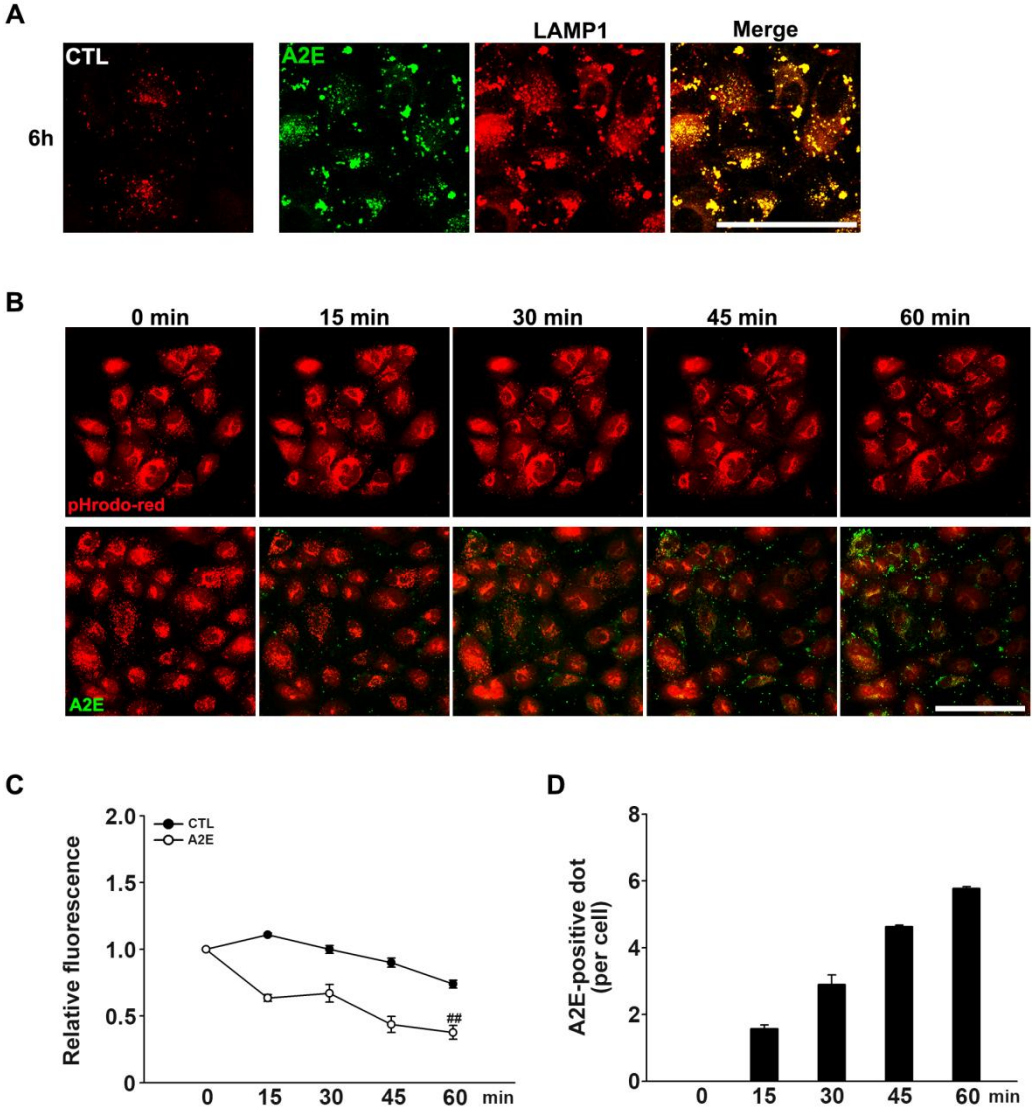

Figure 3. A2E accumulation was localized to the lysosome and reduced the lysosomal acidity

(A) A2E accumulation in lysosomes. Confocal images of the LAMP-1-stained ARPE-19 cells 6 h after treatment with 5 μM A2E. A2E accumulation gradually increased, and the area of accumulation largely overlapped with the lysosomal signals (green: A2E, red: LAMP-1). Original magnification, × 630; scale bar, 100 μm.

(B) Time course of the pH change. Confocal images of pHrodo™ Red-stained ARPE-19 cells treated with A2E. The A2E-treated cells (lower image) showed a decrease in the fluorescence intensity of pHrodo™ Red AM, which further diminished with time compared to the fluorescence intensity in the control cells (upper image). After the addition of 5 μM A2E, the A2E accumulation increased in a time-dependent manner in the ARPE-19 cells (green dots). Original magnification, × 400; scale bar 100 μm.

(C) Quantification of the fluorescence intensity. The graph shows the quantification of the fluorescence of pHrodo™ Red AM in (B) as determined using an ROI analysis (n = 7, $^{\#\#}P < 0.001$).

(D) Quantification of A2E accumulation. The bars denote the relative amount of green dots representing intracellular A2E accumulation (n = 6).

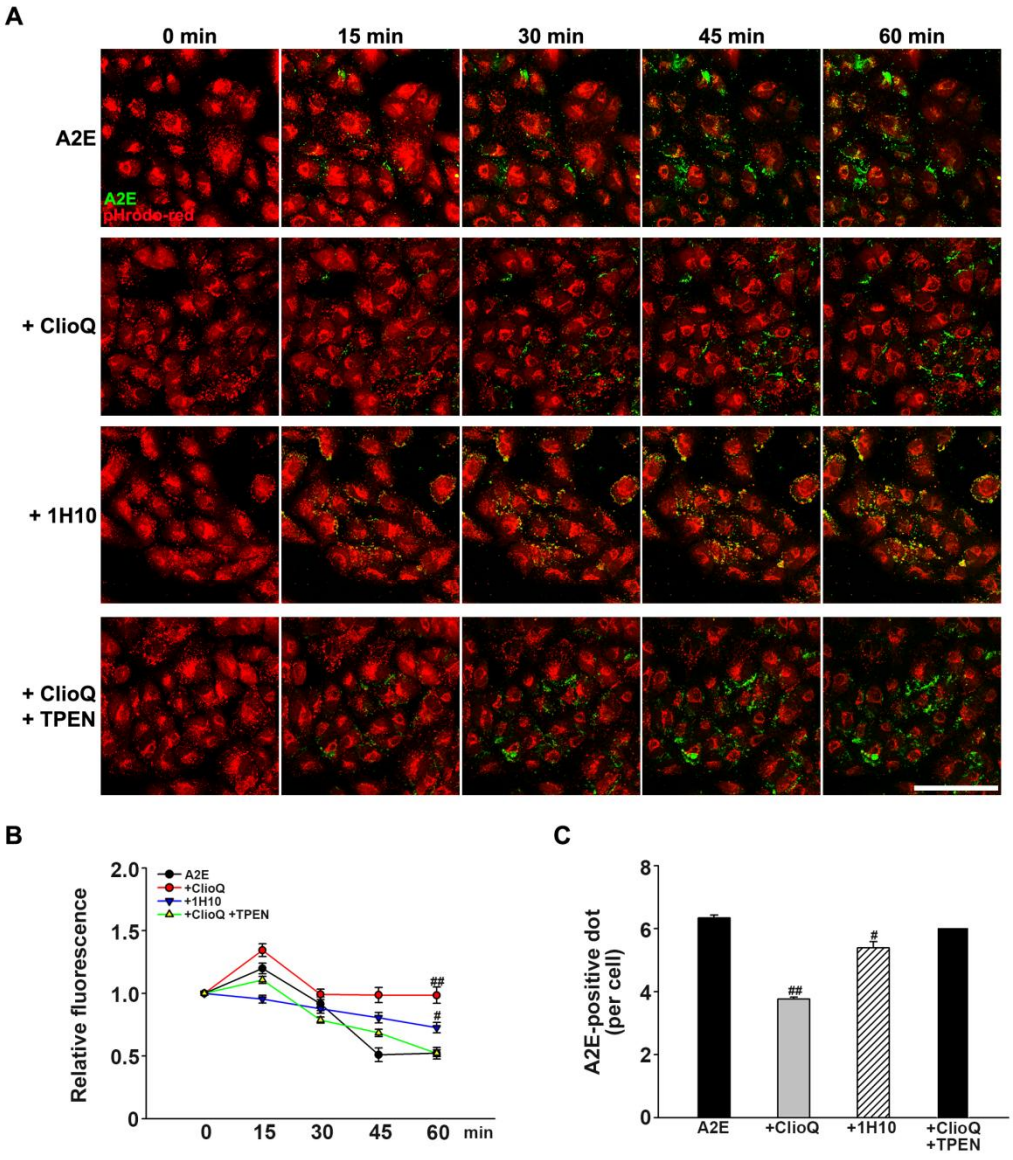

Figure 4. Lysosome re-acidification from treatment with zinc in ARPE-19 cells

(A) Time course of the pH change. Confocal images of the pHrodo™ Red AM stained ARPE-19 cells. ClioQ or 1H10 restored the lysosomal pH to the acidic range, and the chelation of zinc with TPEN completely abolished the effect of ClioQ on the lysosomal pH. Additionally, treatment with A2E plus ClioQ (1 μM) or 1H10 (1 μM) markedly reduced the A2E accumulation. Original magnification, × 630; scale bar

100 μm.

(B) Quantification of the fluorescence intensity. The graph shows the quantification of the fluorescence of pHrodo™ Red AM in (B), determined using an ROI analysis (n = 10, $^{\#}P < 0.005$, $^{\#\#}P < 0.001$).

(C) Quantification of the A2E accumulation. Bars denote the relative number of green dots representing intracellular A2E accumulation (compared to A2E, n = 6, $^{\#}P < 0.005$, $^{\#\#}P < 0.001$).

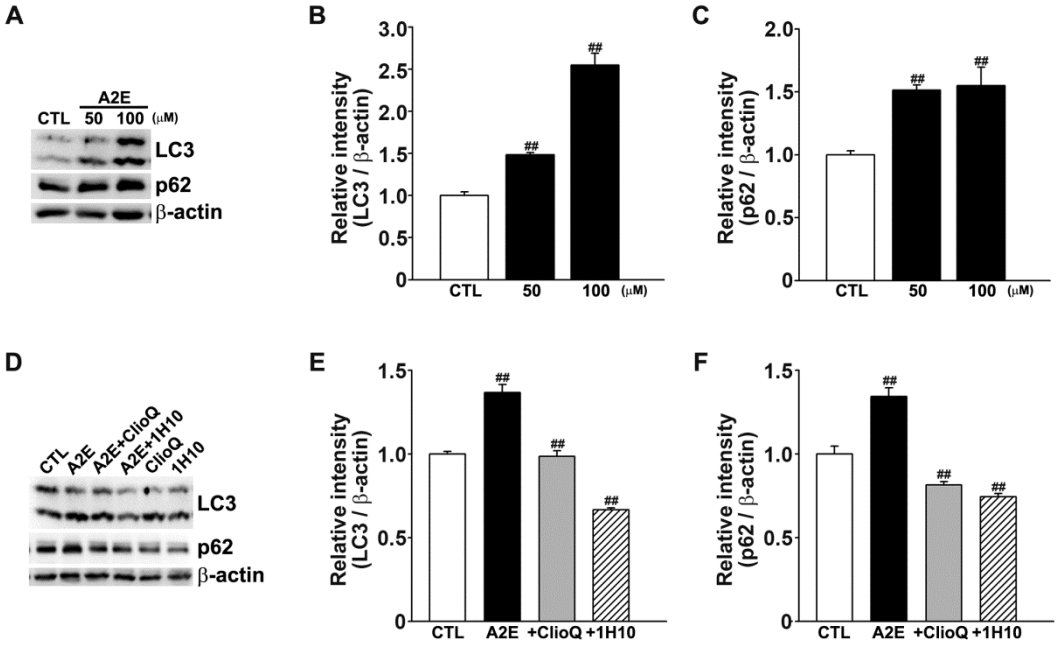

Figure 5. Arrested autophagy from lysosomal dysfunction in A2E-treated ARPE-19 Cells

(A) Measurement of the autophagy flux in the ARPE-19 cells treated with A2E. Western blot analysis showed that LC3-II and p62 increased 3 h after treatment with A2E.

(B) Quantification of the LC3 expression and (C) p62 autophagy flux protein levels from the western blot (n = 3, $^{\#\#}P < 0.001$).

(D) The autophagy markers decreased in the zinc-treated cells. Treatment with 1 μM of ClioQ or 1 μM of 1H10 reduced the p62 levels after 3 h compared to treatment with A2E.

(E) Quantification of the LC3 expression and (F) p62 autophagy flux protein levels from the western blot (n = 3, $^{\#\#}P < 0.001$).

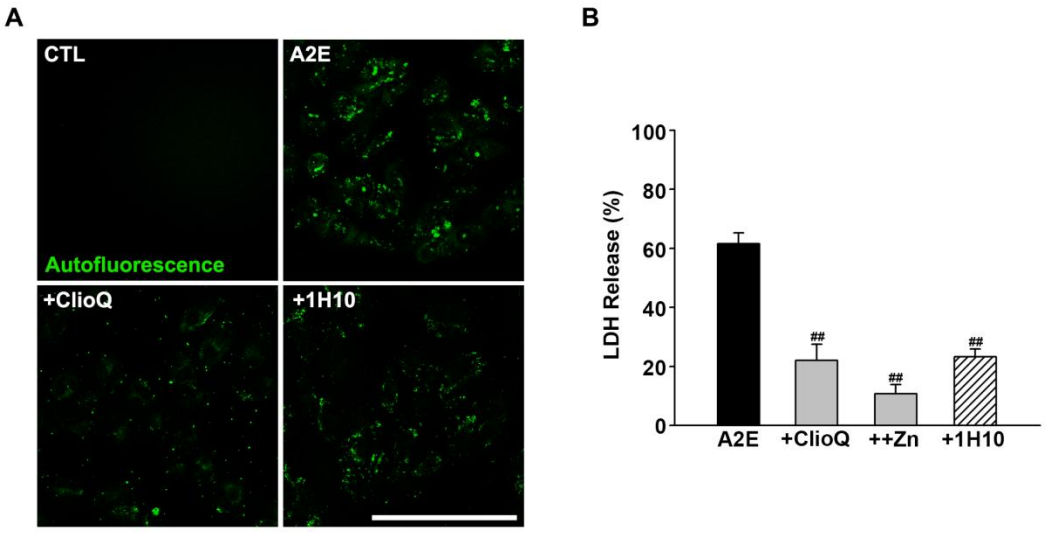

Figure 6. Zinc reduced A2E accumulation and cytotoxicity in RPE cells

(A) Representative images of the ARPE-19 cells treated with A2E. A2E accumulation (autofluorescent dots) increased in the ARPE-19 cells after 3 h. A2E accumulation decreased due to treatment with ClioQ. Additionally, A2E accumulation decreased in the 1H10-treated cells compared to the A2E-treated cells. Original magnification, × 400; scale bar, 200 μm.

(B) Measurement of the LDH released into the medium of the ARPE-19 cells after 24 h of exposure to 5 μM A2E, A2E plus 1 μM of ClioQ, A2E with ClioQ plus 0.5 μM of zinc, or A2E plus 1 μM of 1H10 (compared to the controls, n = 5, $^{\#\#}P <$ 0.001). A2E-induced cell death decreased in the presence of ClioQ or 1H10.

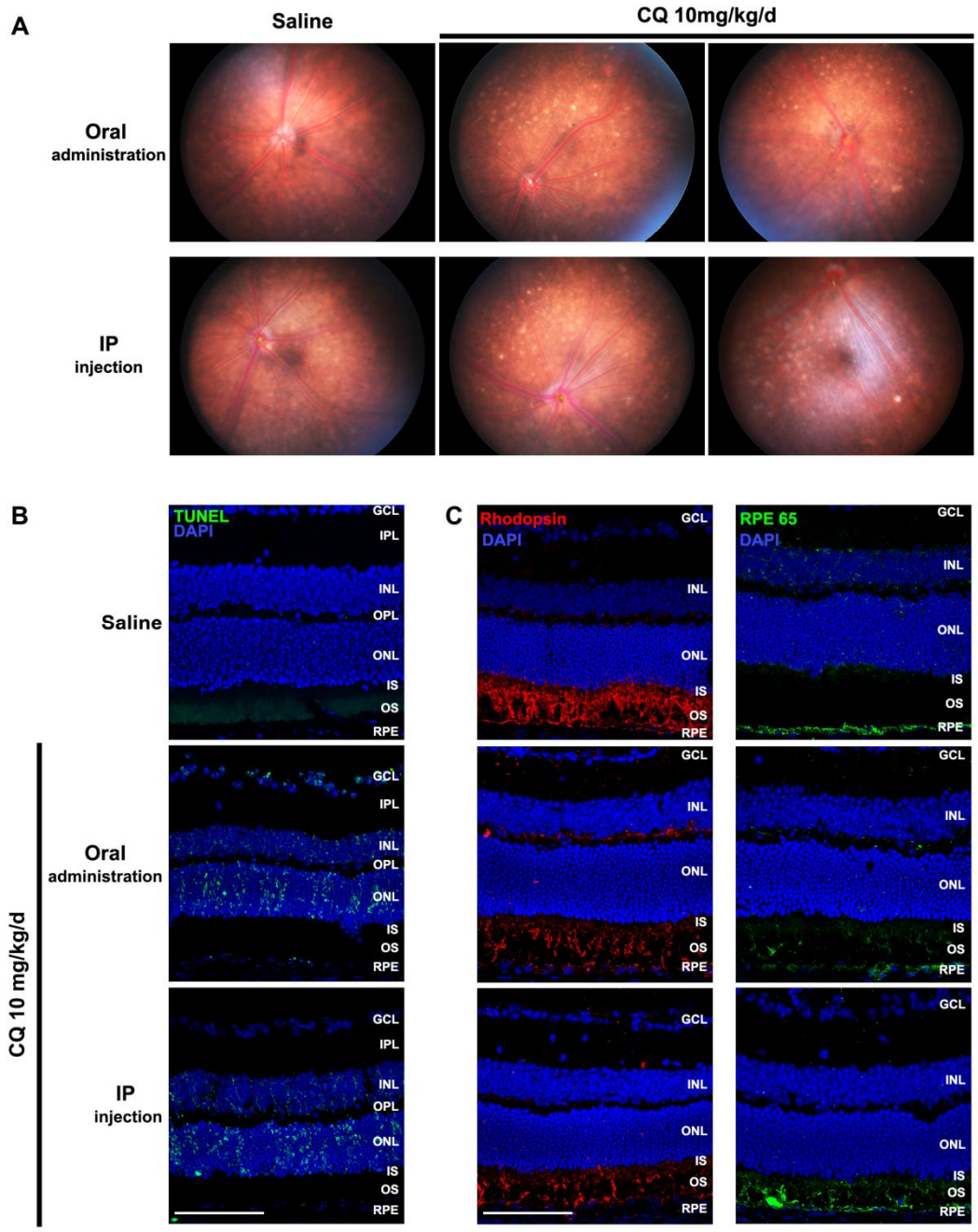

Figure 7. A CQ-induced *in vivo* AMD model in mice

(A) Representative fundus images of the CQ-induced mouse model. Photographs were taken 10 weeks after CQ ip injection (n = 6) or oral administration of CQ (n = 6). The retinas of the CQ-treated mice showed more abnormal white dots in their

RPE compared to the retinas of the control mice (n = 5).

(B) Representative fluorescence photomicrographs of TUNEL-stained retinal tissue sections. The number of TUNEL-positive cells increased markedly in the retinal tissue of both the mice treated with both ip injection and those treated with oral administration of CQ, compared to the saline-treated mice. The TUNEL-positive cells were observed to increase in the outer nuclear layer (ONL) of the retinal tissue of the CQ-treated mice (green: TUNEL; blue: DAPI; n = 4). Original magnification, × 400; scale bar, 100 μm.

(C) Immunohistochemistry of the retinal sections. The CQ-induced mice showed a decrease in the thickness of the RPE and photoreceptor layer. Additionally, the RPE and photoreceptor cell layer had decreased levels of specific protein markers compared to the levels in the saline-treated mice (red: rhodopsin; green: RPE65; blue: DAPI; n = 4). Original magnification, × 400; scale bar, 100 μm.

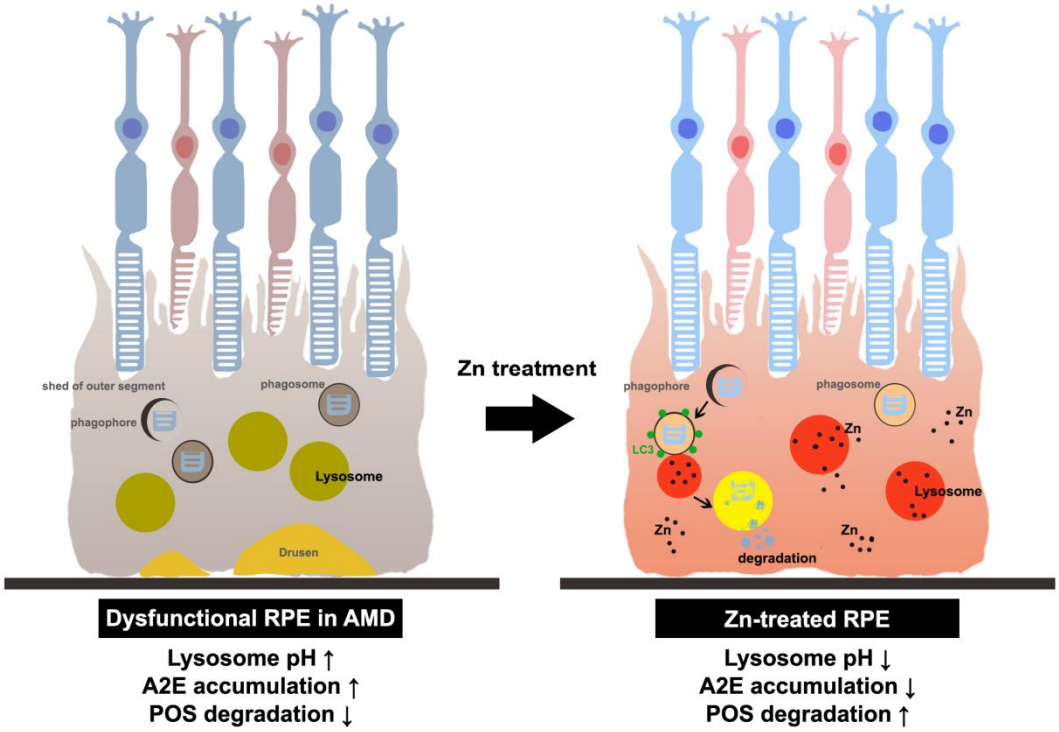

Figure 8. The effects of intracellular zinc on lysosomal alkalization/dysfunction and AMD due to retinal lipofuscin in RPE

Our results demonstrated that raising the intracellular zinc levels can restore the lysosomal acidity and its degradative function in a dysfunctional RPE. We suggest that regulation of the intracellular zinc level may be an important target for AMD treatment.

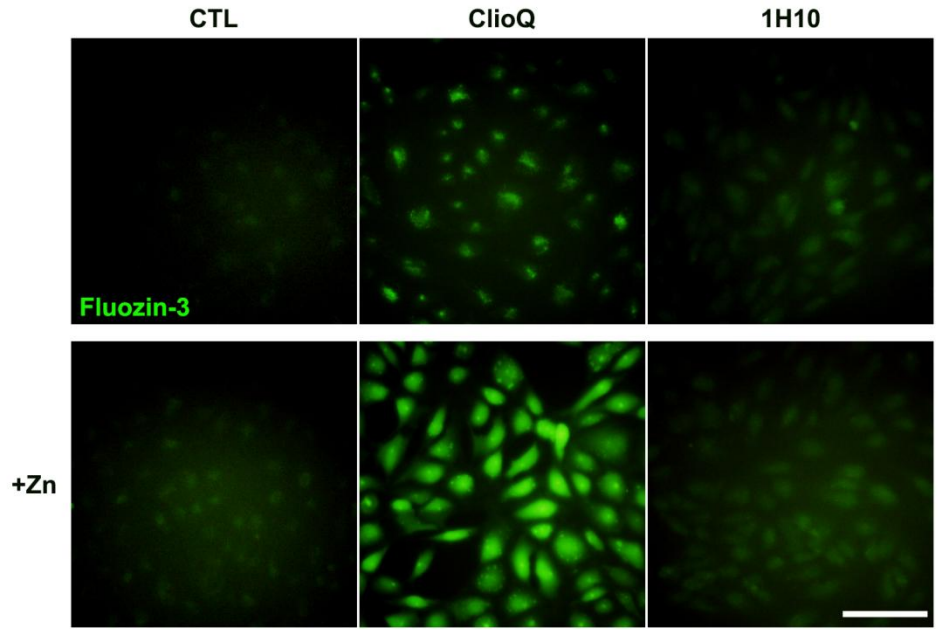

Supplemental Figure 1. Clioquinol and 1H10 act as zinc ionophores

Intracellular zinc staining by use of Fluozin-3 AM (Zn^{2+} selective marker) in ARPE-19 cells. Cells were treated with 1 μM of clioquinol (ClioQ), 1 μM of 1H10, 500 nM of zinc (Zn), clioquinol plus zinc (ClioQ + Zn), or 1H10 plus zinc (1H10 + Zn) for 1 h in normal MEM. ClioQ, a widely used zinc ionophore, and 1H10 increased the intracellular zinc levels in the ARPE-19 cells. The addition of zinc, ClioQ, and 1H10 to the medium significantly increased the intracellular zinc levels. Original magnification, × 400; scale bar, 100 μm.

Discussion

In this study, we showed that the cytotoxic effects of A2E and lysosomal alkalinizing agents, which simulate the pathogenesis of AMD, may be effectively attenuated by zinc treatment to restore the lysosomal pH.

AMD is a complex, multifactorial disease characterized by the degeneration of photoreceptors and retinal pigment epithelial cells[1, 2]. The etiology and pathophysiology of AMD include chronic oxidative stress, decreased choroidal blood flow, and chronic inflammation, and genetic factors are considered to be involved. The molecular hallmark of dry AMD is the accumulation of insoluble extracellular aggregates called drusen, and the deterioration of the proper degradative activity of the RPE cells leads to the accumulation of lipoprotein aggregates[9, 20, 21]. The degradation of lipoprotein aggregates is primarily mediated by lysosomes[17]. Importantly, lysosomal enzymes function optimally within a narrow range of acidic pH values, and the primary degradative enzymes of the RPE reflect the tight dependence on pH. We demonstrated this phenomenon in APRE-19 cells in our current study. We used A2E to verify the dysfunction of the RPE, and A2E accumulation increased in the ARPE-19 cells. The reduced intensity of a lysosomal pH marker was observed in the A2E-treated cells, indicating that A2E induces lysosomal alkalinization.

Some studies have suggested that AMD is similar to common neurodegenerative diseases, such as Alzheimer's disease[22, 23], Parkinson's disease[24, 25], amyotrophic lateral sclerosis, and Huntington's disease, in that these types of disease entities show the accumulation of abnormal protein aggregates. Recently, several studies have reported that zinc treatment increases the functional activity of lysosomes in neurodegenerative diseases[26, 27]. Therefore, considering that dry AMD and neurodegenerative diseases share common pathological mechanisms, the treatment methods used for neurodegenerative diseases may be applicable to the treatment of dry AMD.

We hypothesized that decreasing the lysosomal pH levels with zinc treatment would increase the degradation of lipoproteins and lead to improved RPE function in AMD. ClioQ, a lipophilic compound capable of forming stable complexes with metal ions such as zinc and copper (Ⅱ) is used as a metal chelator that can cross the blood-brain barrier[13, 28]. 1H10, a compound obtained by performing inhibitor screening with the AMPK kinase assay kit, is a substance capable of AMPK inhibition and zinc homeostasis. The function of 1H10 is to regulate zinc as a zinc ionophore, as well as to inhibit zinc toxicity in the cerebral cortex. We used ClioQ or 1H10 as zinc ionophores for experiments in A2E-treated ARPE-19 cells and found that ClioQ and 1H10 reacidified the lysosomal pH and attenuated the A2E accumulation in the A2E-treated ARPE-19 cells. Our results indicate that treatments that induce lysosomal

acidification are important for the prevention of neurotoxicity from abnormal protein accumulation.

Dysfunction of the lysosomal pH is an important characteristic of an AMD model. CQ is a relatively safe drug with good efficacy under clinical conditions and in reports of chloroquine retinopathy. CQ diffuses into acidic vesicles where it becomes protonated and trapped, thereby raising the pH[14]. Considering the decades of documentation of chloroquine retinopathy in patients and the propensity of chloroquine to accumulate in pigmented cells and impair POS degradation, chloroquine is a suitable drug to be used to examine the consequences of the lysosomal alkalization of RPE cells in AMD models[11, 14, 19]. We used a mouse-specified imaging system, MICRON Ⅲ, to confirm the induction of AMD by chloroquine and to examine the differences between experimental groups; we observed abnormal white dots in the retinas of CQ-injected mice, representing mutated RPE. Additionally, we observed RPE cell death and damage to the RPE layer in the retinal sections of the CQ-treated mice. These results suggest the possibility that CQ-treated mice can serve as a disease model for dry AMD.

In conclusion, the present study demonstrates that adequate levels of zinc may help to overcome the cytotoxic effects of A2E or lysosomal alkalinizing agents, both of which may contribute to the pathogenesis of AMD.

References

1. Bonilha VL. Age and disease-related structural changes in the retinal pigment epithelium. Clin Ophthalmol 2008;2(2):413-24.
2. Ambati J, Fowler BJ. Mechanisms of age-related macular degeneration. Neuron 2012;75(1):26-39.
3. Bowes Rickman C, Farsiu S, Toth CA, Klingeborn M. Dry age-related macular degeneration: mechanisms, therapeutic targets, and imaging. Invest Ophthalmol Vis Sci 2013;54(14):ORSF68-80.
4. Zajac-Pytrus HM, Pilecka A, Turno-Krecicka A, Adamiec-Mroczek J, Misiuk-Hojlo M. The Dry Form of Age-Related Macular Degeneration (AMD): The Current Concepts of Pathogenesis and Prospects for Treatment. Adv Clin Exp Med 2015;24(6):1099-104.
5. Zarbin MA. Current concepts in the pathogenesis of age-related macular degeneration. Arch Ophthalmol 2004;122(4):598-614.
6. Mazzoni F, Safa H, Finnemann SC. Understanding photoreceptor outer segment phagocytosis: use and utility of RPE cells in culture. Exp Eye Res 2014;126:51-60.
7. Liu J, Lu W, Reigada D, Nguyen J, Laties AM, Mitchell CH. Restoration of lysosomal pH in RPE cells from cultured human and ABCA4(-/-) mice: pharmacologic approaches and functional recovery. Invest Ophthalmol Vis Sci 2008;49(2):772-80.
8. Bosch E, Horwitz J, Bok D. Phagocytosis of outer segments by retinal pigment epithelium: phagosome-lysosome interaction. J Histochem Cytochem 1993;41(2):253-63.
9. Guha S, Liu J, Baltazar G, Laties AM, Mitchell CH. Rescue of compromised lysosomes enhances degradation of photoreceptor outer segments and reduces lipofuscin-like autofluorescence in retinal pigmented epithelial cells. Adv Exp Med Biol 2014;801:105-11.
10. Mitter SK, Rao HV, Qi X, Cai J, Sugrue A, Dunn WA, Jr., et al. Autophagy in the

retina: a potential role in age-related macular degeneration. Adv Exp Med Biol 2012;723:83-90.

11. Guha S, Coffey EE, Lu W, Lim JC, Beckel JM, Laties AM, et al. Approaches for detecting lysosomal alkalinization and impaired degradation in fresh and cultured RPE cells: evidence for a role in retinal degenerations. Exp Eye Res 2014;126:68-76.

12. Guha S, Baltazar GC, Coffey EE, Tu LA, Lim JC, Beckel JM, et al. Lysosomal alkalinization, lipid oxidation, and reduced phagosome clearance triggered by activation of the P2X7 receptor. FASEB J 2013;27(11):4500-9.

13. Seo BR, Lee SJ, Cho KS, Yoon YH, Koh JY. The zinc ionophore clioquinol reverses autophagy arrest in chloroquine-treated ARPE-19 cells and in APP/mutant presenilin-1-transfected Chinese hamster ovary cells. Neurobiol Aging 2015;36(12):3228-38.

14. Yoon YH, Cho KS, Hwang JJ, Lee SJ, Choi JA, Koh JY. Induction of lysosomal dilatation, arrested autophagy, and cell death by chloroquine in cultured ARPE-19 cells. Invest Ophthalmol Vis Sci 2010;51(11):6030-7.

15. Choi JA, Kim YJ, Seo BR, Koh JY, Yoon YH. Potential Role of Zinc Dyshomeostasis in Matrix Metalloproteinase-2 and -9 Activation and Photoreceptor Cell Death in Experimental Retinal Detachment. Invest Ophthalmol Vis Sci 2018;59(7):3058-68.

16. Arnault E, Barrau C, Nanteau C, Gondouin P, Bigot K, Vienot F, et al. Phototoxic action spectrum on a retinal pigment epithelium model of age-related macular degeneration exposed to sunlight normalized conditions. PLoS One 2013;8(8):e71398.

17. Sparrow JR, Parish CA, Hashimoto M, Nakanishi K. A2E, a lipofuscin fluorophore, in human retinal pigmented epithelial cells in culture. Invest Ophthalmol Vis Sci 1999;40(12):2988-95.

18. Bjorkoy G, Lamark T, Brech A, Outzen H, Perander M, Overvatn A, et al. p62/SQSTM1 forms protein aggregates degraded by autophagy and has a protective effect on huntingtin-induced cell death. J Cell Biol 2005;171(4):603-14.

19. Lee DH, Melles RB, Joe SG, Lee JY, Kim JG, Lee CK, et al. Pericentral hydroxychloroquine retinopathy in Korean patients. Ophthalmology 2015;122(6):1252-6.
20. Golestaneh N, Chu Y, Xiao YY, Stoleru GL, Theos AC. Dysfunctional autophagy in RPE, a contributing factor in age-related macular degeneration. Cell Death Dis 2017;8(1):e2537.
21. Inana G, Murat C, An W, Yao X, Harris IR, Cao J. RPE phagocytic function declines in age-related macular degeneration and is rescued by human umbilical tissue derived cells. J Transl Med 2018;16(1):63.
22. Kaarniranta K, Salminen A, Haapasalo A, Soininen H, Hiltunen M. Age-related macular degeneration (AMD): Alzheimer's disease in the eye? J Alzheimers Dis 2011;24(4):615-31.
23. Biscetti L, Luchetti E, Vergaro A, Menduno P, Cagini C, Parnetti L. Associations of Alzheimer's disease with macular degeneration. Front Biosci (Elite Ed) 2017;9:174-91.
24. Chung SD, Ho JD, Hu CC, Lin HC, Sheu JJ. Increased risk of Parkinson disease following a diagnosis of neovascular age-related macular degeneration: a retrospective cohort study. Am J Ophthalmol 2014;157(2):464-9 e1.
25. Mahyar Etminan AS, Bonnie He. Risk of Parkinson’s disease in patients with neovascular age-related macular degeneration. Journal of Current Ophthalmology 2018;In press.
26. Lee SJ, Koh JY. Roles of zinc and metallothionein-3 in oxidative stress-induced lysosomal dysfunction, cell death, and autophagy in neurons and astrocytes. Mol Brain 2010;3(1):30.
27. Lee SJ, Park MH, Kim HJ, Koh JY. Metallothionein-3 regulates lysosomal function in cultured astrocytes under both normal and oxidative conditions. Glia 2010;58(10):1186-96.
28. Di Vaira M, Bazzicalupi C, Orioli P, Messori L, Bruni B, Zatta P. Clioquinol, a drug for Alzheimer's disease specifically interfering with brain metal metabolism: structural characterization of its zinc(II) and copper(II) complexes. Inorg Chem

2004;43(13):3795-7.

Korean Abstract

건성 연령 관련 황반변성 (Dry-AMD)은 드루젠 (dusen)이라 불리는 불용성 세포 외 응집체의 축적과 광수용체 세포 (photoreceptor)와 망막색소상피 세포 (retinal pigment epithelial cell, RPE)의 퇴행을 특징으로 한다. RPE 세포에서 lysosome 의 기능이 망가지면 shedding 된 광수용체 세포 outer segments 의 분해가 억제되어 RPE 에 침착 되어 건성 황반 변성의 병리학에 기여한다고 보고되어왔다. 우리의 이전 연구결과에서 세포 내 아연 수준을 높이면 lysosome 의 산성도와 분해기능을 회복시킬 수 있음을 확인 하였다. 본 연구에서는 건성 황반 변성의 세포모델에서 아연이 lysosome 알칼리화 및 기능 장애에 미치는 영향을 조사 하였다.

인간 망막색소상피 세포주 (ARPE19)에서 lysosome 기능 장애를 유도하기 위해 우리는 A2E (lipofuscin derivative)를 사용했다. 우리는 A2E 로 유도 된 세포 사멸을 LDH assay 를 이용하여 정량적으로 평가했다. A2E 를 처리하고 24 시간 후, ARPE19 세포는 상당한 양의 세포 사멸을 보였다. A2E 의 축적을 확인하고 lysosome 의 pH 변화를 확인하기 위해 공초점 라이브 이미징 시스템과 pHrodo ™ Red-AM (약산성이 되면 형광신호가 감소하는 pH 측정 염색)을 사용하여 측정 하였다. A2E 처리 한 세포는 대조군 세포와 비교하여 세포에서 A2E 가 축적되고 동시에 pHrodo ™ Red 형광신호를 감소 시키는 것을 보여 주었다. 또한, 아연 아이오노포어인 ClioQ 와 1H10 을 처리한 세포에서는 A2E 의 축적을 감소시키고 lysosome pH 를 산성 범위로 회복시켰다. 아연 아이노포어를 처리한 세포군 에서는 자식작용이 활성화 되었고,

A2E- 유도 된 세포 사멸도 현저하게 감소되었다. A2E 처리된 ARPE19 세포에서 아연이 lysosome 의 산성화를 강화시켜 축적된 A2E 분해 기능을 향상 시킬 수 있음을 확인하였다.

우리의 연구결과는 적절한 수준의 아연이 AMD 의 병인에 기여하는 A2E 로 인한 독성 또는 lysosome 의 약산성화를 극복하는 데 도움이 될 가능성을 확인하였다.

Key words: 건성 연령 관련 황반변성, 망막색소상피 세포, 라이소좀, 아연, 인간 망막색소상피 세포주